Full Paper

# Design, Synthesis, and Anticancer Properties of Novel Benzophenone-Conjugated Coumarin Analogs

**V. Lakshmi Ranganatha[1], Farhan Zameer[2], S. Meghashri[3], N. D. Rekha[4], V. Girish[1], H. D. Gurupadaswamy[1], and Shaukath Ara Khanum[1]**

[1] Department of Chemistry, Yuvaraja's College, University of Mysore, Mysore, Karnataka, India
[2] Mahajana Life Science Research Laboratory, Department of Biotechnology, Microbiology and Biochemistry, Mahajana Research Foundation, Pooja Bhagavat Memorial Mahajana Post-Graduate Centre, Affiliated to University of Mysore, Metagalli, Mysore, Karnataka, India
[3] Pronet Informatics Pvt. Ltd, Bangalore, Karnataka, India
[4] Department of Studies in Biotechnology, JSS College of Arts, Commerce and Science, Mysore, Karnataka, India

In the current scenario, development of anticancer drugs with specific targets is of prime importance in modern chemical biology. Observing the importance of benzophenone and coumarin nucleus, it would be worthwhile to design and synthesize novel benzophenone derivatives (**8a–o**) bearing the coumarin nucleus. Further, they were screened for prospective anticancer activities *in vitro* against the Michigan Cancer Foundation-7 (MCF-7) and Ehrlich's ascites tumor (EAT) cell lines and their biomarkers, followed by *in silico* studies regarding phosphoinositide 3-kinase (PI3K) and caspase by molecular docking. Benzophenones have been reported as potential drugs targeting tumor angiogenesis; thus, the formation of neovessels in an *in vivo* model system like CAM, which is angiogenesis dependent, was observed in the presence of compounds **8a–o**. The above findings would help in understanding their putative potential as therapeutic agents for cancer patients.

**Keywords:** Anticancer agents / Benzophenone / CAM / Caspase / Coumarin / PI3K / Structure–activity relation (SAR)

Received: August 10, 2013; Revised: September 1, 2013; Accepted: September 5, 2013

DOI 10.1002/ardp.201300298

## Introduction

Cancer, the second cause of mortality in the world, is continuing to be a major health hazard in developing as well as in undeveloped countries [1]. Design and development of anticancer drugs with fewer or no side effects are important for the treatment of cancer. The search for such potential anticancer drugs has led to the discovery of synthetic molecules with anticarcinogenic activity. Therefore cancer has become a major challenge to mankind [2], and it has opened up myriad new avenues for advance drug design and discoveries.

In continuation of our previous research toward the development of antiangiogenic as well as anticancer drugs [3–6], more specifically benzophenone derivatives, [2-(4-methoxy-benzoyl)-4-methylphenoxy]-*N*-(4-chloro-phenyl)-acetamide (BP-1, $IC_{50}$: 42.50 μM) was known to inhibit angiogenesis. It prevents the angiogenesis-dependent disorders like mammary carcinoma and rheumatoid arthritis both *in vivo* and *in vitro*, where it down-regulated the vascular endothelial growth factor (VEGF) gene expression, which is responsible for angiogenesis. Herein, we report the synthesis of potential antiangiogenic molecules by combining two bioactive molecules like benzophenone and coumarin collectively through amide linkage to achieve pharmacologically efficacious single molecules. In order to develop novelty in cancer therapy, recently our group developed new benzophenone-integrated oxadiazole analogs as potent anticancer drugs [6]. Developing angiogenesis inhibitors is a desirable anticancer target, which minimizes the side effects caused by the chemotherapy. Specificity in selecting tumor

**Correspondence:** Dr. Shaukath Ara Khanum, Department of Chemistry, Yuvaraja's College, University of Mysore, Mysore 570 005, Karnataka, India.
**E-mail:** shaukathara@yahoo.co.in
**Fax:** +91 821 2419239

endothelial cells and neovessel formation as a target by drugs is their unique property, which could be developed into potential antiangiogenic drug for cancer therapeutics [7, 8].

Moreover, benzophenones are a class of compounds obtained from natural source [9] or by synthetic methods [10]. . They are of great importance fundamentally due to their diverse biological and chemical properties. Benzophenones exhibit significant antitumor activity both *in vitro* and *in vivo* [11]. In addition, synthetic benzophenones, such as 2-aminobenzophenone [12] and dihydroxy-4-methoxy benzophenone [13], have proven to be antimitotic and anticancer agents, respectively. Recently, *para*-methoxy substituted benzophenones were evaluated as p38a inhibitors with high efficacy and selectivity ($IC_{50}$: 14 nM) [14]. Amino and methoxy substituted benzophenones have been reported to be potent cytotoxic agents against a panel of human cancer cell lines including multi-drug-resistant cell lines [15]. Analogs of benzophenone exhibit a selective toxicity for proliferating endothelial cells by induction of apoptosis [16], and polyprenylated benzophenone derivatives are also able to induce caspase-mediated apoptosis [17].

In addition, coumarin derivatives have been found to exhibit a wide range of biological and controlled therapeutic activities in view of their extensive occurrence and also due to low toxicity [18]. Furthermore, they are present in natural and synthetic compounds possessing biological activity, effective and specific at different stages of cancer formation. Some of them have cytostatic properties and the others have cytotoxic activity [19]. A few naturally occurring coumarins have been found to exhibit cytotoxicity against a panel of mammalian cancer cell lines [20].

In continuation of our present and previous work, further motivated by the above-mentioned biological properties, an effort was made to achieve new coumarin-conjugated benzophenone derivatives. Herein, we report the synthesis, angiogenesis, and anticancer activity of new coumarin incorporated benzophenones on Michigan Cancer Foundation-7 (*MCF-7*) and Ehrlich's ascites tumor (EAT) cancer cell lines and also caspase and phosphoinositide 3-kinase (PI3K) enzyme regulation pathways. Further, this study was also supported by *in silico* molecular docking. Hence, the results of this study will hold promising pavement for developing a safer alternative to the existing anticancer agents.

## Results and discussion

### Chemistry

Synthesis of the title compounds **8a–o** was accomplished by a synthetic procedure as shown in Scheme 1. All the synthesized compounds were confirmed by IR and proton NMR data. In IR spectra of benzoylated products **3a–o**, the appearance of O=C (carbonyl) stretching band for ester group and in proton NMR, the disappearance of broad singlet for OH proton of substituted phenols **1a–c** indicate the formation of compounds **3a–o**. Fries rearrangement of compounds **3a–o** gave hydroxy benzophenones **4a–o**, which were confirmed by the disappearance of O–C stretching band and appearance of O–H stretching band in IR spectra and by the appearance of broad singlet for OH proton and decrease in one aromatic proton in proton NMR. Compounds **4a–o** on etherification with chloro ethylacetate gave substituted ethyl esters **5a–o**, which was confirmed by disappearance of O–H stretching band and appearance of O=C (carbonyl) stretching band for ester group in IR absorption spectra. The proton NMR observations reveal the disappearance of broad singlet for OH proton and appearance of triplet and quartet for $CH_3$ and $CH_2$ protons, respectively. The substituted ethyl esters **5a–o** on treatment with 99% hydrazine hydrate yield (4-benzoyl phenoxy)-aceto hydrazides **6a–o**, which was clearly evident with the appearance of N–H and $NH_2$ stretching bands in IR spectra. In proton NMR, the appearance of NH and $NH_2$ protons and disappearance of triplet and quartet peaks for $CH_3$ and $CH_2$ protons confirm the formation of product. Finally all the substituted aceto hydrazides, on treatment with coumarin-3-carboxylic acid (**7**) in the presence of TBTU and lutidine as a coupling reagent, deliver the expected final products **8a–o** in a good yield. These final products are more assertively confirmed by NMR, IR, mass, and CHN analyses by concurring the expected data with experimentally determined data indistinguishably.

### Pharmacology

#### *Preliminary screening of compounds 8a–o*

In the present study, the cytotoxic effect of compounds **8a–o** was investigated on MCF-7 breast cancer cell lines following 48-h exposure using Trypan blue and (3-(4,5-dimethylthiazol-2-yl)-2,5-diphenyltetrazolium bromide (MTT). This method is opted as a first target screening method to eliminate those analogs that do not show any cytotoxic effects. In this screening, tamoxifen was used as a standard and dimethyl sulfoxide (DMSO) as negative control, and the results are reported in Table 1. In the Trypan blue assay, the analogs **8d**, **8l**, and **8o** reveal excellent cell growth inhibition when compared to the standard with $IC_{50}$ of 7.7, 9.4, 10.4, and 11.4 μM, respectively. Furthermore, the effect of compounds **8a–o** on cell proliferation was tested using MTT assay. The results observed in MTT assay were concurrent with Trypan blue (Table 1). The compounds **8d**, **8l**, and **8o** showed maximum cytotoxicity with an $IC_{50}$ value of 7.6, 9.3, and 10.2, respectively, followed by standard tamoxifen ~11.4 μM. It is obvious from the data that compound **8d** with bromo group at *ortho* position of phenyl ring exhibited highest activity against MCF-7 cells in Trypan blue and MTT assay with the $IC_{50}$

 

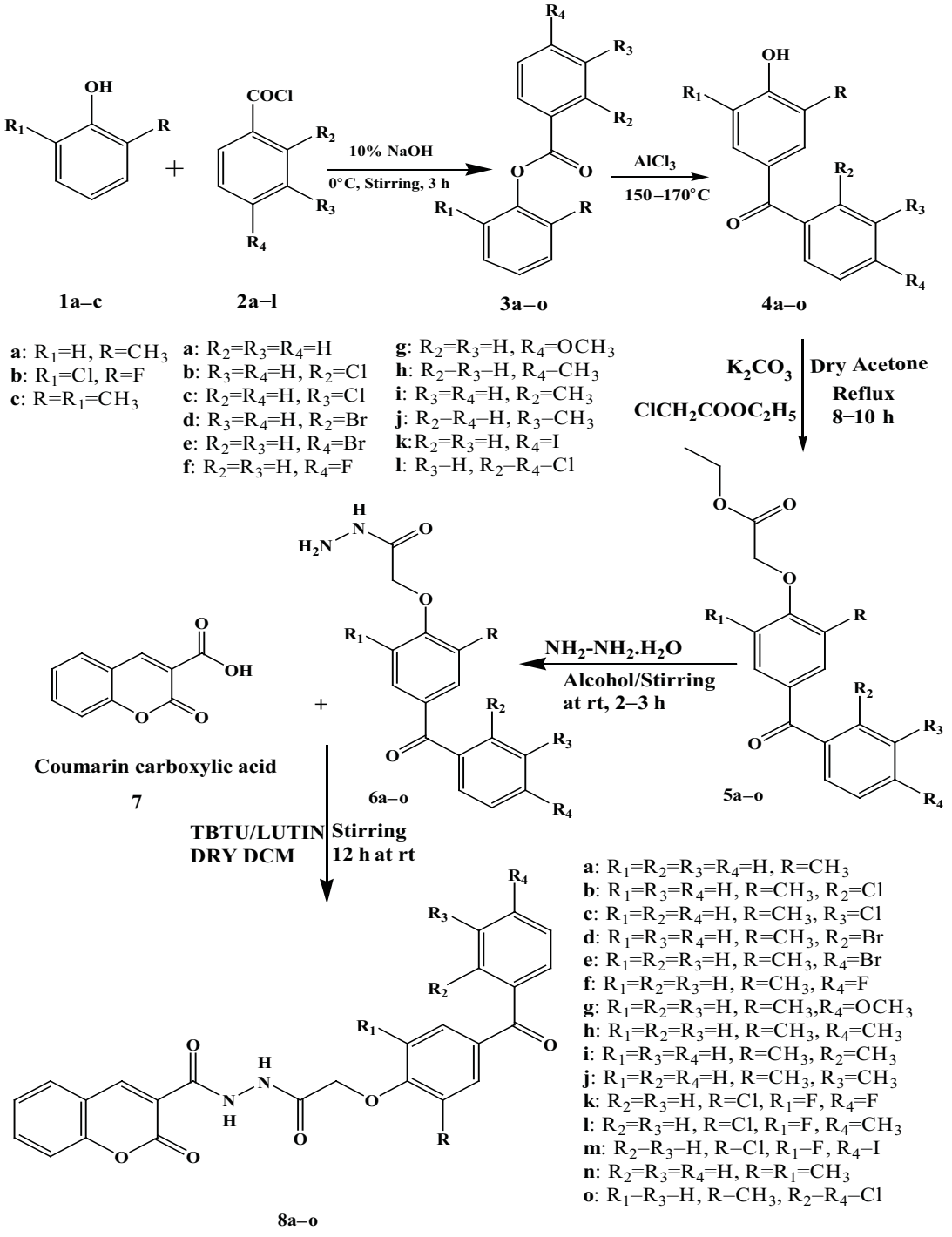


**Scheme 1.** Synthesis of benzophenone-conjugated coumarin analogs.

values of 7.7 and 7.6 μM when compared with the standard drug with an $IC_{50}$ of 11.4 μM, followed by moderate activity of 9.4 and 9.3 μM, 10.4 and 10.2 μM by compounds **8l** with chloro and fluoro groups at *ortho* position of phenoxy ring and methyl group at *para* position of benzoyl ring and **8o** with two chloro groups at *ortho* position of phenoxy ring, respectively. In order to elucidate the mode of action of cell death, the best three synthesized analogs **8d**, **8l**, and **8o** were evaluated for

 

**Table 1.** $IC_{50}$ values of compounds **8a–o** calculated based on Trypan blue and MTT assay at 48 h in MCF-7 cells.

| Compounds | Trypan blue assay $IC_{50}$ value (μM) | MTT assay $IC_{50}$ value (μM) |
|---|---|---|
| Control | – | – |
| **8a** | 98 ± 0.11 | >100 |
| **8b** | 29 ± 0.19 | 26 ± 0.18 |
| **8c** | 69 ± 0.13 | 71 ± 0.14 |
| **8d** | **7.7** ± 0.09 | **7.6** ± 0.10 |
| **8e** | >100 | >100 |
| **8f** | 46 ± 0.15 | 48 ± 0.17 |
| **8g** | 75 ± 0.18 | 73 ± 0.13 |
| **8h** | >100 | >100 |
| **8i** | 57 ± 0.14 | 56 ± 0.13 |
| **8j** | 72 ± 0.17 | 72 ± 0.15 |
| **8k** | 20 ± 0.10 | 21 ± 0.13 |
| **8l** | **9.4** ± 0.02 | **9.3** ± 0.04 |
| **8m** | >100 | >100 |
| **8n** | 80 ± 0.20 | 84 ± 0.21 |
| **8o** | **10.4** ± 0.08 | **10.2** ± 0.12 |
| Std | **11.4** ± 0.06 | **11.4** ± 0.09 |

The $IC_{50}$ values of compounds **8d**, **8l**, and **8o** (values in bold) were very significant; thus, **8d**, **8l**, and **8o** were chosen as lead compounds.

their effects on homogeneous caspase and PI3-kinase in MCF-7 cell line. Hence, the compounds **8d**, **8l**, and **8o** were selected as lead compounds and further investigated.

## Compounds 8d, 8l, and 8o considered as potent molecules

### *Angiogenesis in CAM model*

To investigate the antiangiogenic activity of compounds **8a–o** in *in vivo* models, all the compounds **8a–o** were subjected to CAM angiogenesis assay. In this model, the compounds **8a–o** induced moderate-to-good avasculture zone formation in the developing embryos. Among all the tested compounds, compounds **8d**, **8l**, and **8o** more clearly showed regression of newly formed microvessels, which were found around the area of disk implanted, compared to the other compounds in the series (Fig. 1A). This regression of microvessels density in the CAM model is highly evident for the tumor inhibition and it correlates to our *in vitro* results more accurately.

### *Giemsa and ethidium bromide/acridine orange staining*

To study the morphological features of the cells, we subjected the cells to Giemsa and ethidium bromide/acridine orange

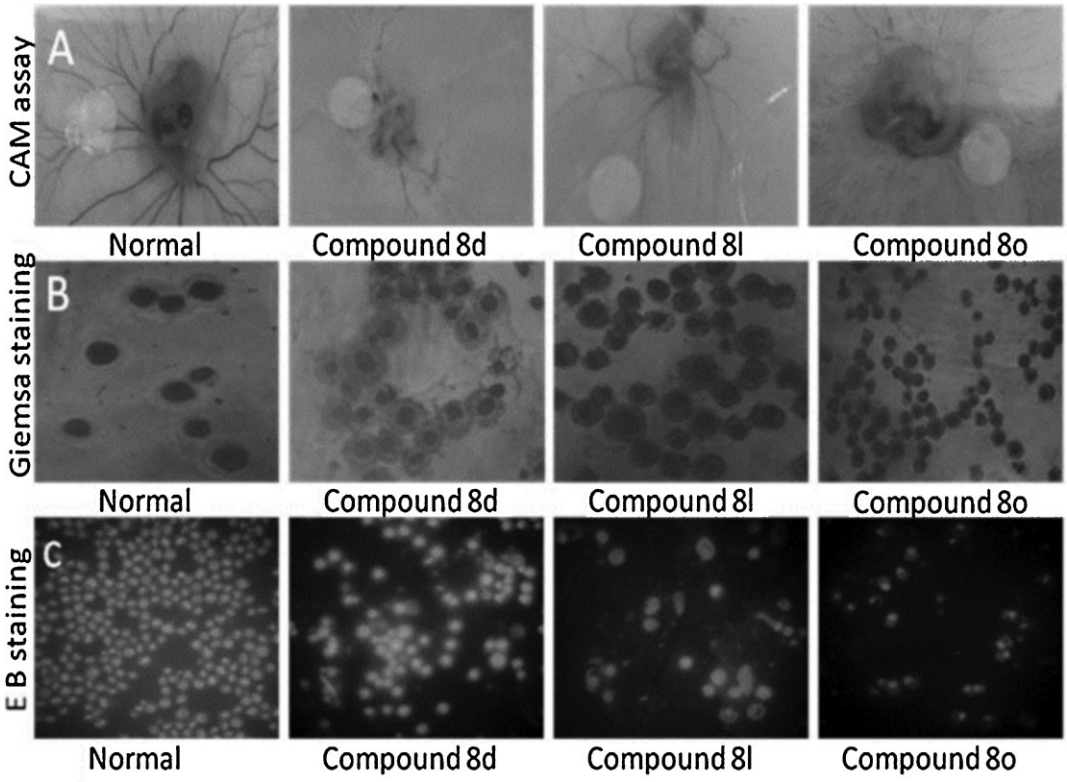


**Figure 1.** Angioprevention effect of compounds **8d**, **8l**, and **8o**. (A) CAM photos illustrate the formation of blood vessels in normal cells followed by regression in cells treated with compounds **8d**, **8l**, and **8o**. Inhibition of angiogenesis is evident. (B) Giemsa staining of normal cells and cells treated with compounds **8d**, **8l**, and **8o** highlights the apoptotic morphology of the cells. (C) Representative photographs clearly indicating apoptotic morphology of cells treated with compounds **8d**, **8l**, and **8o** and stained with ethidium bromide/acridine orange stain.

 

staining. In this, experimental batches of both test and control smears were stained with Giemsa's stain and acridine orange/ethidium bromide stain that highlights the apoptotic morphology of the cells, when observed under florescent microscope (Fig. 1B and C). The apoptotic morphology clearly indicated the potential of the compounds **8d**, **8l**, and **8o**, respectively, and the same were photographed.

### *DNA fragmentation assay*

DNA fragmentation was performed for elucidating the mode of action of the investigated compounds, especially with respect to induction of oligonucleosomal DNA fragmentation (DNA ladder), which is a characteristic feature of the programmed cell death or apoptosis. Apoptotic degradation of DNA was analyzed by agarose gel electrophoresis. The fragmented DNA observed under UV light clearly demonstrated the *in vivo* apoptotic effect of compounds **8d**, **8l**, and **8o**. In the clearly documented Bio-RAD image (Fig. 2), lane 1 indicates control, lane 2 indicates the marker, and lanes 3–5 indicate the apoptotic effect of compounds **8d**, **8l**, and **8o**, respectively. These results have greater resemblance to our other *in vitro* and *in vivo* results. Further by observing these facts, we can conclude that the compounds **8d**, **8l**, and **8i** had more proapoptotic properties when compared to all other analogs in the series.

### *Caspase and PI3-kinase activation assay*

In order to elucidate the mode of action of cell death, the best three synthesized analogs **8d**, **8l**, and **8o** were evaluated for their effects on homogeneous caspase and PI3-kinase in MCF-7 cells. The result indicates that the homogeneous caspase activity was increased in MCF-7 cells by these three compounds. The caspase activity upon treatment of respective compounds was significantly high compared to untreated control, indicating that all these compounds activated general caspases (Fig. 3) indicating benzophenone-integrated coumarin analogs, which induced apoptosis via caspase activation. These results were further confirmed by *in silico* analysis for looking into structure–activity relationship for which the three major caspases, namely 1, 3, and 8, were considered and molecular docking was carried out.

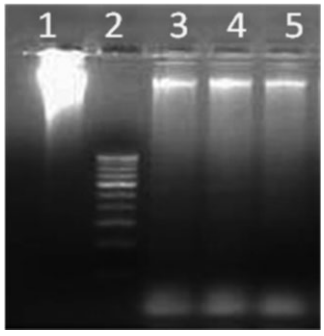


**Figure 2.** DNA fragmentation assay. The fragmented DNA observed under UV light clearly demonstrated the *in vivo* apoptotic effect of the compounds. Lanes 1 and 2 are control and marker, lanes 3–5 are compounds **8d**, **8l**, and **8o**, respectively.

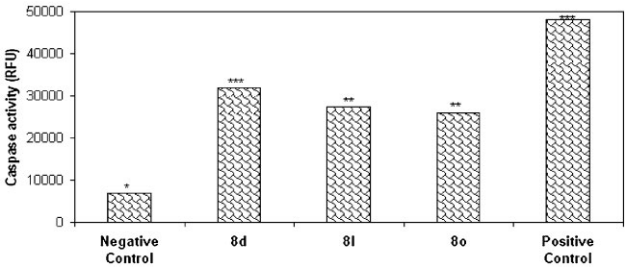


**Figure 3.** Title compounds activate homogeneous caspase in MCF-7 cells: $1 \times 10^4$ cells/well with 70–80% confluence were grown for 24 h, treated with 5 μM of each compounds. Flurometric determination of general caspase was done as described in Materials and Methods section with an excitation filter of 465 nm and emission filter of 520 nm ($^*p < 0.05$ vs. negative control).

In the mean time, all the conjugates were tested for PI3K enzyme inhibition in MCF-7 cells treated at a concentration of 5 μM. This also exhibited the promising results, indicating the potency of the inhibitors used. As mentioned earlier, PI3-kinases have a pivotal role in signaling pathways involved in oncogenic transformation and intracellular protein trafficking. The benzophenone-integrated coumarin derivatives induced apoptosis via PI3K triggering. Mainly the compounds **8d**, **8l**, and **8o** showed significant inhibition against PI3K (Fig. 4). An increased activity in MCF-7 cells by all the three compounds **8d**, **8l**, and **8o** is outstanding.

## *In silico* modeling of compounds 8d, 8l, and 8o with caspase and PI3-kinase enzymes

Molecular docking of homogeneous caspase results revealed the atomic contact energy (ACE) and amino acid binding residues, which are depicted in Table 2. This analysis

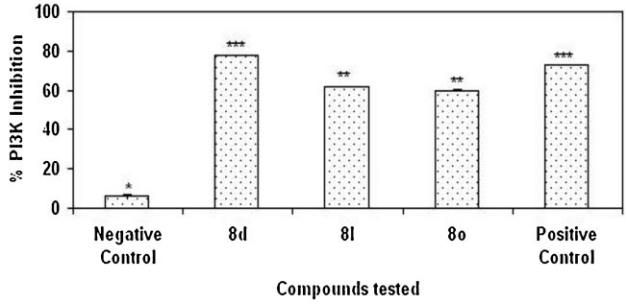


**Figure 4.** Enzyme inhibition of PI3K in MCF-7 cells treated at a concentration of 5 μM.

 

**Table 2.** Molecular docking results exhibiting atomic contact energy (ACE) values and amino acid residues binding pockets for analyzed caspases against the synthesized ligand molecules.

| | Caspase-1 (PDB: 2HBZ) | | Caspase-3 (PDB: 4DCP) | | Caspase-8 (PDB: 1QDU) | |
|---|---|---|---|---|---|---|
| **Compound** | **ACE** | **Amino acid residues** | **ACE** | **Amino acid residues** | **ACE** | **Amino acid residues** |
| **8d** | **−163.29** | Glu 250 | **−212.44** | Arg 207 | −83.01 | Lys 253 |
| | | Ser 339 | | Glu 123 | | Asp 319 |
| | | Cys 285 | | Cys 163 | | Cys 360 |
| | | Arg 341 | | | | Asp 363 |
| **8l** | −131.23 | Gln 142 | −195.39 | Glu 123 | −77.37 | Asp 455 |
| | | Ile 152 | | Cys 163 | | Gln 423 |
| | | | | | | Lys 457 |
| **8o** | −117.91 | Lys 158 | −212.27 | Lys 82 | **−138.76** | Asp 319 |
| | | Gln 142 | | Asp 228 | | Cys 360 |
| | | | | Lys 224 | | Asp 363 |
| Std | **−235.58** | Ile 176 | **−242.14** | Cys 163 | **−217.26** | Asp 319 |
| | | Cys 285 | | Tyr 204 | | Cys 360 |
| | | Asp 288 | | Arg 207 | | Ser 411 |

along with previous studies on caspases proves that they are cysteine-dependent aspartate-directed proteases that mediate programmed cell death (apoptosis) and involve both the extrinsic and intrinsic pathways, among which caspase 1 is an interleukin-1 beta converting enzyme (ICE) homolog. Caspase 8 is an initiator caspase, which forms part of the death-inducing signaling complex (DISC) once a death signal is received by the cell. The formation of this complex allows for the autocatalytic cleavage of procaspases into active caspases. Activated caspases allow for the activation of the effector caspases, including caspase 3. The SAR also supports the above data, which is evident by the docking results and the docked amino acid pockets (Fig. 5) mainly indicating the presence of Cys-Asp-Glu-Gln residues. Taken

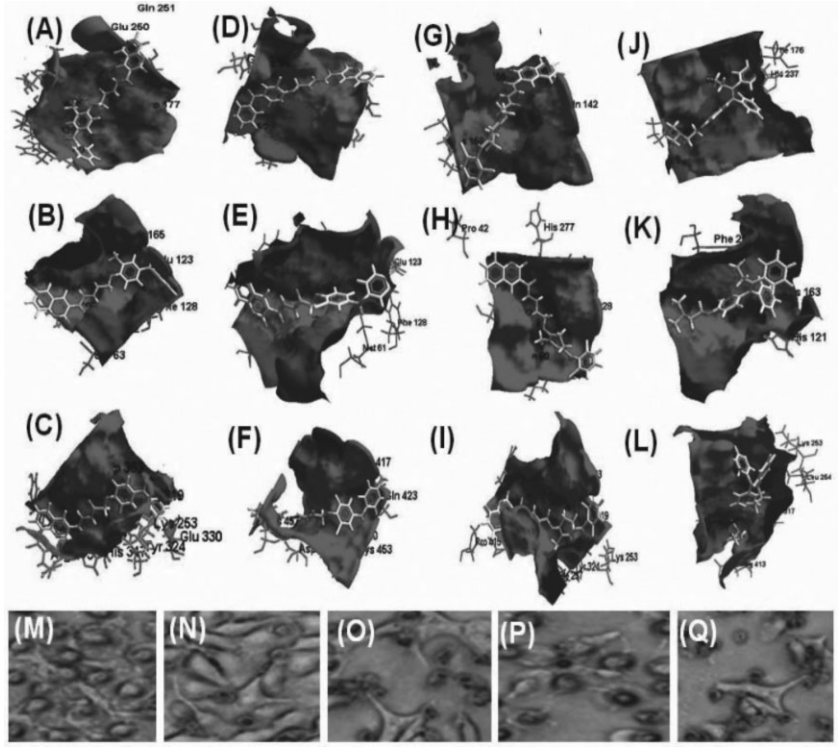


**Figure 5.** Molecular docking of human caspase 1, 3, and 8 receptor with ligand **8d** (A–C), with **8l** (D–F), with **8o** (G–I), and with standard tamoxifen (J–L) indicating site of dock of the ligand to amino acid residues.

 

**Table 3.** Molecular docking results exhibiting ACE values, amino acid residues binding pockets for analyzed human PI3K against the synthesized ligand molecules.

| Compound | ACE values | Amino acid residues | Domain | Function |
|---|---|---|---|---|
| PI3K + **8d** | −434.28 | Val 540, His 541, Arg 542 | PI3K_C2 superfamily | Chemotaxis and interference in PI3K metabolism and ATP binding activity in cytosol and membrane bound region |
| PI3K + **8l** | −428.35 | Val 540 | PI3K_C2 superfamily | ATP binding activity |
| PI3K + **8o** | −417.53 | Trp 539, Arg 542, Phen 545 | PI3K_C2 superfamily | Interference in small molecule metabolic process a nd PI3K signaling pathways |
| PI3K + Std | −408.22 | Val 540, His 541 | PI3K_C2 superfamily | ATP binding activity and chemotaxis |

Our docking region: 506–629, indicating PI3K_C2 super family.

together, the above results demonstrate that the synthesized benzophenone-integrated coumarin analogs have potential anticancer properties and are mainly directed by caspase-induced apoptosis mechanism.

In the meantime, the *in silico* model of compounds **8d**, **8l**, and **8o** was studied and the results of molecular docking with ACE values with PI3K inhibition are tabulated in Table 3. The docking studies and compound microscopic images further strengthen the evidence to the *in vitro* results. Here the docking results of compounds **8d**, **8l**, and **8o** are extremely similar to that of standard tamoxifen with amino acid packets (Fig. 6). The above result shows that the different substitutions at respective positions of the main skeleton of compounds **8a–o** may enhance the biological activity.

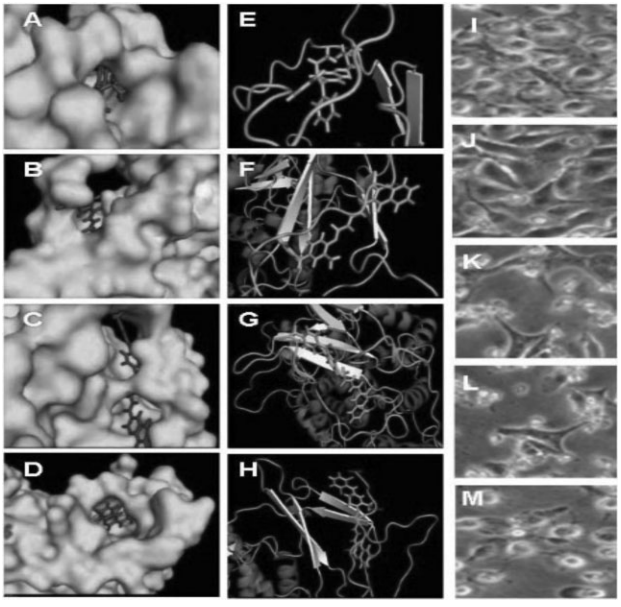


**Figure 6.** (A–D) Molecular surface of docking in the order Std, compounds **8d**, **8l**, and **8o**. (E–H) Amino acid pockets and (I–M) are the compound microscopic images, which indicates the effect of 5 μM concentration of potent inhibitors starting from untreated cells, Std, compounds **8d**, **8l**, and **8o**, respectively.

## Conclusion

In order to develop novel anticancer molecules, we have designed and synthesized new bioactive benzophenone-integrated coumarin analogs (**8a–o**) and evaluated them for anticancer properties. The anticancer activity of these compounds was tested against MCF-7 cells by different methods. Compounds **8d**, **8l**, and **8o** exhibited potent anticancer properties among the series. *In silico* results are also concordant with *in vitro* and *in vivo* results more accurately. Further *in vivo* investigations are in progress in our laboratory. By observing the present results, the compounds **8d**, **8l**, and **8o** can be considered as potent anticancer drugs for future chemotherapy.

## Experimental

All solvents and reagents were purchased from Sigma–Aldrich Chemicals Pvt Ltd. Melting points were determined on an electrically heated VMP-III melting point apparatus. The elemental analysis of the compounds was performed on a Perkin Elmer 2400 elemental analyzer. The FT-IR spectra were recorded using KBr disks and Nujol on FT-IR Jasco 4100 infrared spectrophotometer. The $^{1}$H NMR spectra were recorded using Bruker DRX 400 spectrometer at 400 MHz with TMS as the internal standard. Mass spectra were recorded on LC–MS/MS (API-4000) mass spectrometer.

### Synthesis and characterization

The reaction sequence for different title compounds (**7a–o**) is outlined in Scheme 1. The starting materials substituted phenyl benzoates (**3a–o**) were synthesized according to a reported procedure [21] through the reaction of substituted phenols (**1a–c**) with substituted acid chlorides (**2a–l**) in the presence of 10% sodium hydroxide. The phenyl benzoates (**3a–o**) on subjecting to Fries rearrangement afforded hydroxy benzophenones (**4a–o**). Ethyl (2-aroyl-4 methylphenoxy) acetates (**5a–o**) were achieved in excellent yield by reacting compounds **4a–o** with ethyl

 

chloroacetate in the presence of anhydrous potassium carbonate and dry acetone. Compounds **5a–o** treated with 99% hydrazine hydrate gave different hydrazides (**6a–o**). Finally, compounds **6a–o** on coupling with coumarin 3-carboxylic acid (**7**) in the presence of *O*-(benzotriazol-1-yl)-*N*,*N*,*N*′,*N*′-tetramethyl uronium tetrafluoroborate (TBTU) and 2,6-dimethyl pyridine (lutidine) as a coupling agent furnished **8a–o** in excellent yield.

### *General procedure for the preparation of phenyl benzoates (3a–o)*

Substituted benzoates (**3a–o**) were synthesized by benzoylation of substituted phenols (**1a–c**) with corresponding benzoyl chlorides (**2a–l**, 1:1) using 10% sodium hydroxide solution. The reaction mass was stirred for 2–3 h at 0°C. Reaction was monitored by thin layer chromatography (TLC) using 4:1 *n*-hexane/ethyl acetate solvent mixture. After completion of the reaction the oily product was extracted with ether layer. Ether layer was washed with 10% sodium hydroxide solution ($3 \times 50$ mL) followed by water ($3 \times 30$ mL) and then dried over anhydrous sodium sulfate and the solvent was evaporated under pressure to afford compounds **3a–n**. Compound **3a** is taken as a representative example to explain characterization data [21].

**3a**: Yield 90%. Pale yellow liquid; IR (Nujol): 1715 $cm^{-1}$ (C=O); $^1H$ NMR ($CDCl_3$): $\delta$ 2.45 (s, 3H, Ar–$CH_3$), 7.0–8.2 (m, 9H, Ar–H). Anal. calcd. for $C_{14}H_{12}O_2$ (212): C, 79.22; H, 5.70. Found: C, 79.18; H, 5.76%.

### *General procedure for the preparation of (4-hydroxy phenyl)phenyl-methanones (4a–o)*

Substituted (4-hydroxy phenyl)phenyl-methanones commonly known as hydroxy benzophenones (**4a–o**) were synthesized by Fries rearrangement. Compounds **3a–o** (0.001 mol) were treated with anhydrous aluminum chloride (0.002 mol) as a catalyst at 150–170°C without solvent for about 2–3 h. Then the reaction mixture was cooled to room temperature and quenched with 6 N HCl in the presence of ice water. The reaction mixture was stirred for about 2–3 h; solid was filtered and recrystallized with methanol to obtain compounds **4a–o**. Compound **4a** is taken as a representative example to explain characterization data [22].

**4a**: Yield 72%. m.p. 110–112°C; IR: (Nujol) 1640 (C=O), 3510–3600 $cm^{-1}$ (OH); $^1H$ NMR ($CDCl_3$): $\delta$ 2.35 (s, 3H, $CH_3$), 6.71–7.70 (m, 8H, Ar–H), 12.0 (bs, 1H, –OH). Anal. calcd. data for $C_{14}H_{12}O_2$ (212.08): C, 79.22; H, 5.70. Found: C, 72.23; H, 5.69%.

### *General procedure for the preparation of ethyl(4-benzoyl phenoxy)aceto esters (5a–o)*

Compounds **5a–o** were obtained by refluxing a mixture of compounds **4a–n** (0.013 mol) and ethyl chloroacetate (0.026 mol) in dry acetone (50 mL) and anhydrous potassium carbonate (0.019 mol) for 8–9 h. The reaction mixture was cooled and solvent was removed by distillation. The residual mass was triturated with cold water to remove potassium carbonate and extracted with ether ($3 \times 50$ mL). The ether layer was washed with 10% sodium hydroxide solution ($3 \times 50$ mL) followed by water ($3 \times 30$ mL) and then dried over anhydrous sodium sulfate and evaporated to dryness to obtain crude solid, which, on recrystallization with ethanol, afforded compounds **5a–n**. Compound **5a** is taken as a representative example to explain characterization data [23].

**5a**: Yield 90%. m.p. 49–52°C; IR (Nujol): 1664 (C=O), 1760 $cm^{-1}$ (ester, C=O); $^1H$ NMR ($CDCl_3$): $\delta$ 1.2 (t, 3H, $CH_3$ of ester), 2.3 (s, 3H, $CH_3$), 4.1 (q, 2H, $CH_2$ of ester), 4.5 (s, 2H, $OCH_2$), 7.1–7.7 (m, 8H, Ar–H). Anal. calcd. for $C_{18}H_{18}O_4$ (298): C, 72.48; H, 6.04. Found: C, 72.46; H, 6.02%.

### *General procedure for the preparation of (4-benzoyl phenoxy)aceto hydrazides (6a–o)*

To compounds **5a–o** (0.01 mol) in ethanol (10 mL), 99% hydrazine hydrate (0.01 mol) was added dropwise and continuously stirred for 2 h at room temperature to achieve white solid compounds **6a–o**. Solid was recrystallized with methanol to get pure products (**6a–o**). Compound **6a** is taken as a representative example to explain characterization data [24].

**6a**: Yield 80%. m.p. 125–128°C; IR (Nujol): 1630 (C=O), 1670 (amide, C=O), 3120–3220 $cm^{-1}$ (NH $NH_2$); $^1H$ NMR ($CDCl_3$): $\delta$ 2.2 (s, 3H, Ar–$CH_3$), 4.35 (bs, 2H, $NH_2$), 4.63 (s, 2H, $CH_2$), 6.96–7.68 (m, 8H, Ar–H), 9.30 (bs, $^1H$, CONH). Anal. calcd. for $C_{16}H_{16}N_2O_3$ (285): C, 67.59; H, 5.67; N, 9.85. Found: C, 67.65; H, 5.74; N, 9.91%.

### *General procedure for the preparation of 2-oxo-2H-chromene-3-carboxylic acid N′-[2-(4-benzoyl-2-methyl-phenoxy)-acetyl]-hydrazide derivatives (8a–o)*

To the mixture of compounds **6a–o** (0.0037 mol) in dry dichloromethane (15 mL), lutidine (1.2 vol.) was added at 25–30°C followed by coumarin 3-carboxylic acid (**7**, 0.0037 mol) and stirred at 25–30°C for 30 min. The reaction mass was cooled to 0–5°C and TBTU (0.0037 mol) was added in lots over a period of 30 min by maintaining temperature below 5°C. The reaction mass was stirred overnight and monitored by TLC using chloroform/methanol (9:1). The reaction mass was diluted with 20 mL of dichloromethane followed by 1.5 N HCL solution (20 mL). The organic layer was washed with water (25 mL), dried over anhydrous sodium sulfate, concentrated to syrupy liquid, and recrystallized twice by diethyl ether to afford compounds **8a–o**.

### *2-Oxo-2H-chromene-3-carboxylic acid N′-[2-(4-benzoyl-2-methyl-phenoxy)acetyl]-hydrazide*

**8a**: Yield 85%. m.p. 190–193°C; IR (Nujol): 1630 (C=O), 1670 (amide C=O), 3120–3220 $cm^{-1}$ (NH–NH); $^1H$ NMR ($CDCl_3$): $\delta$ 2.2 (s, 3H, Ar–$CH_3$), 4.8 (s, 2H, $CH_2$), 7.0–8.0 (m, 12H, Ar–H), 8.9 (s, 1H, coumarin Ar–H), 10.5–10.9 (d, 2H, –NHNH); MS: *m*/*z* 476. Anal. calcd. for $C_{26}H_{20}N_2O_6$: C, 68.42; H, 4.42; N, 6.14. Found: C, 68.45; H, 4.44; N, 6.19%.

### *2-Oxo-2H-chromene-3-carboxylic acid N′-{2-[4-(2-chloro-benzoyl)-2-methyl-phenoxy]-acetyl}-hydrazide*

**8b**: Yield 88%. m.p. 200–202°C; IR (Nujol): 1620 (C=O), 1675 (amide C=O), 3140–3250 $cm^{-1}$ (NH–NH); $^1H$ NMR ($CDCl_3$): $\delta$ 2.4 (s, 3H, Ar–$CH_3$), 4.6 (s, 2H, $CH_2$), 7.1–8.0 (m, 11H, Ar–H), 8.8 (s, 1H, coumarin Ar–H), 10.6–10.9 (d, 2H, –NHNH); MS: *m*/*z* 511. Anal. calcd. for $C_{26}H_{19}ClN_2O_6$: C, 63.61; H, 3.90; N, 5.71. Found: C, 63.68; H, 3.99; N, 5.80%.

### *2-Oxo-2H-chromene-3-carboxylic acid N′-{2-[4-(3-chloro-benzoyl)-2-methyl-phenoxy]-acetyl}-hydrazide*

**8c**: Yield 80%. m.p. 180–185°C; IR (Nujol): 1620 (C=O), 1675 (amide C=O), 3140–3250 $cm^{-1}$ (NH–NH); $^1H$ NMR ($CDCl_3$): $\delta$ 2.4 (s, 3H,

 

Ar–$CH_3$), 4.6 (s, 2H, $CH_2$), 7.1–8.0 (m, 11H, Ar–H), 8.7 (s, 1H, coumarin Ar–H), 10.4–10.9 (d, 2H, –NHNH); MS: *m/z* 491. Anal. calcd. for $C_{26}H_{19}ClN_2O_6$: C, 63.61; H, 3.90; N, 5.71. Found: C, 63.68; H, 3.97; N, 5.80%.

### *2-Oxo-2H-chromene-3-carboxylic acid N′-{2-[4-(2-bromo-benzoyl)-2-methyl-phenoxy]-acetyl}-hydrazide*

**8d**: Yield 85%. m.p. 202–205°C; IR (Nujol): 1625 (C=O), 1675 (amide C=O), 3130–3240 $cm^{-1}$ (NH–NH); $^1H$ NMR ($CDCl_3$): $\delta$ 2.5 (s, 3H, Ar–$CH_3$), 4.3 (s, 2H, $CH_2$), 7.2–8.1 (m, 11H, Ar–H), 8.9 (s, 1H, coumarin Ar–H), 10.4–10.9 (d, 2H, –NHNH); MS: *m/z* 536. Anal. calcd. for $C_{26}H_{19}BrN_2O_6$: C, 58.33; H, 3.58; N, 5.23. Found: C, 58.40; H, 3.65; N, 5.29%.

### *2-Oxo-2H-chromene-3-carboxylic acid N′-{2-[4-(4-bromo-benzoyl)-2-methyl-phenoxy]-acetyl}-hydrazide*

**8e**: Yield 80%. m.p. 210–212°C; IR (Nujol): 1625 (C=O), 1675 (amide C=O), 3130–3240 $cm^{-1}$ (NH–NH); $^1H$ NMR ($CDCl_3$): $\delta$ 2.5 (s, 3H, Ar–$CH_3$), 4.3 (s, 2H, $CH_2$), 7.1–8.0 (m, 11H, Ar–H), 8.6 (s, 1H, coumarin Ar–H), 10.6–10.9 (d, 2H, –NHNH); MS: *m/z* 536. Anal. calcd. for $C_{26}H_{19}BrN_2O_6$: C, 58.33; H, 3.58; N, 5.23. Found: C, 58.40; H, 3.65; N, 5.29%.

### *2-Oxo-2H-chromene-3-carboxylic acid N′-{2-[4-(4-fluoro-benzoyl)-2-methyl-phenoxy]-acetyl}-hydrazide*

**8f**: Yield 82%. m.p. 225–228°C; IR (Nujol): 1625 (C=O), 1675 (amide C=O), 3130–3240 $cm^{-1}$ (NH–NH); $^1H$ NMR ($CDCl_3$): $\delta$ 2.5 (s, 3H, Ar–$CH_3$), 4.3 (s, 2H, $CH_2$), 7.1–8.0 (m, 11H, Ar–H), 8.9 (s, 1H, coumarin Ar–H), 10.4–10.9 (d, 2H, –NHNH); MS: *m/z* 475. Anal. calcd. for $C_{26}H_{19}FN_2O_6$: C, 65.82; H, 4.04; N, 5.90. Found: C, 65.88; H, 4.10; N, 5.97%.

### *2-Oxo-2H-chromene-3-carboxylic acid N′-{2-[4-(4-methoxy-benzoyl)-2-methyl-phenoxy]-acetyl}-hydrazide*

**8g**: Yield 90%. m.p. 197–199°C; IR (Nujol): 1625 (C=O), 1675 (amide C=O), 3130–3240 $cm^{-1}$ (NH–NH); $^1H$ NMR ($CDCl_3$): $\delta$ 2.2 (s, 3H, Ar–$CH_3$), 3.7 (S, 3H, $OCH_3$), 4.3 (s, 2H, $CH_2$), 6.7–7.9 (m, 11H, Ar–H), 8.6 (s, 1H, coumarin Ar–H), 10.5–10.9 (d, 2H, –NHNH); MS: *m/z* 487. Anal. calcd. for $C_{27}H_{22}N_2O_7$: C, 66.66; H, 4.56; N, 5.76. Found: C, 66.70; H, 4.59; N, 5.80%.

### *2-Oxo-2H-chromene-3-carboxylic acid N′-{2-[2-methyl-4-(4-methyl-benzoyl)-phenoxy]-acetyl}-hydrazide*

**8h**: Yield 85%. m.p. 188–191°C; IR (Nujol): 1625 (C=O), 1675 (amide C=O), 3130–3240 $cm^{-1}$ (NH–NH); $^1H$ NMR ($CDCl_3$): $\delta$ 2.2 (s, 3H, Ar–$CH_3$), 2.5 (S, 3H, $CH_3$), 4.3 (s, 2H, $CH_2$), 7.3–8.2 (m, 11H, Ar–H), 8.9 (s, 1H, coumarin Ar–H), 10.4–10.9 (d, 2H, –NHNH); MS: *m/z* 471. Anal. calcd. for $C_{27}H_{22}N_2O_6$: C, 68.93; H, 4.71; N, 5.95. Found: C, 68.99; H, 4.77; N, 5.96%.

### *2-Oxo-2H-chromene-3-carboxylic acid N′-{2-[2-methyl-4-(2-methyl-benzoyl)-phenoxy]-acetyl}-hydrazide*

**8i**: Yield 78%. m.p. 178–180°C; IR (Nujol): 1625 (C=O), 1675 (amide C=O), 3130–3240 $cm^{-1}$ (NH–NH); $^1H$ NMR ($CDCl_3$): $\delta$ 2.2 (s, 3H, Ar–$CH_3$), 2.4 (S, 3H, $CH_3$), 4.4 (s, 2H, $CH_2$), 7.2–8.2 (m, 11H, Ar–H), 8.8 (s, 1H, coumarin Ar–H), 10.4–10.9 (d, 2H, –NHNH); MS: *m/z* 471. Anal. calcd. for $C_{27}H_{22}N_2O_6$: C, 68.93; H, 4.71; N, 5.95. Found: C, 68.99; H, 4.77; N, 5.96%.

### *2-Oxo-2H-chromene-3-carboxylic acid N′-{2-[2-methyl-4-(3-methyl-benzoyl)-phenoxy]-acetyl}-hydrazide*

**8j**: Yield 80%. m.p. 200–204°C; IR (Nujol): 1625 (C=O), 1675 (amide C=O), 3130–3240 $cm^{-1}$ (NH–NH); $^1H$ NMR ($CDCl_3$): $\delta$ 2.2 (s, 3H, Ar–$CH_3$), 2.3 (S, 3H, $CH_3$), 4.1 (s, 2H, $CH_2$), 7.3–8.3 (m, 11H, Ar–H), 8.7 (s, 1H, coumarin Ar–H), 10.4–10.9 (d, 2H, –NHNH); MS: *m/z* 471. Anal. calcd. for $C_{27}H_{22}N_2O_6$: C, 68.93; H, 4.71; N, 5.95. Found: C, 68.99; H, 4.77; N, 5.96%.

### *2-Oxo-2H-chromene-3-carboxylic acid N′-{2-[2-chloro-6-fluoro-4-(4-fluoro-benzoyl)-phenoxy]-acetyl}-hydrazide*

**8k**: Yield 78%. m.p. 207–209°C; IR (Nujol): 1625 (C=O), 1675 (amide C=O), 3130–3240 $cm^{-1}$ (NH–NH); $^1H$ NMR ($CDCl_3$): $\delta$ 4.4 (s, 2H, $CH_2$), 7.2–8.1 (m, 10H, Ar–H), 8.7 (s, 1H, coumarin Ar–H), 10.4–10.9 (d, 2H, –NHNH); MS: *m/z* 514. Anal. cald. for $C_{25}H_{15}ClF_2N_2O_6$: C, 58.55; H, 2.95; N, 5.46. Found: C, 58.59; H, 2.99; N, 5.48%.

### *2-Oxo-2H-chromene-3-carboxylic acid N′-{2-[2-chloro-6-fluoro-4-(4-methyl-benzoyl)-phenoxy]-acetyl}-hydrazide*

**8l**: Yield 88%. m.p. 175–177°C; IR (Nujol): 1625 (C=O), 1675 (amide C=O), 3130–3240 $cm^{-1}$ (NH–NH); $^1H$ NMR ($CDCl_3$): $\delta$ 2.5 (s, 3H, Ar–$CH_3$), 4.4 (s, 2H, $CH_2$), 7.1–8.2 (m, 10H, Ar–H), 8.7 (s, 1H, coumarin Ar–H), 10.4–10.9 (d, 2H, –NHNH); MS: *m/z* 510. Anal. calcd. for $C_{26}H_{18}ClFN_2O_6$: C, 61.37; H, 3.57; N, 5.50. Found: C, 61.42; H, 3.61; N, 5.53%.

### *2-Oxo-2H-chromene-3-carboxylic acid N′-{2-[2-chloro-6-fluoro-4-(4-iodo-benzoyl)-phenoxy]-acetyl}-hydrazide*

**8m**: Yield 85%. m.p. 235–238°C; IR (Nujol): 1625 (C=O), 1675 (amide C=O), 3130–3240 $cm^{-1}$ (NH–NH); $^1H$ NMR ($CDCl_3$): $\delta$ 4.2 (s, 2H, $CH_2$), 7.3–8.4 (m, 10H, Ar–H), 8.5 (s, 1H, coumarin Ar–H), 10.4–10.9 (d, 2H, –NHNH); MS: *m/z* 622. Anal. calcd. for $C_{25}H_{15}ClFIN_2O_6$: C, 48.37; H, 2.44; N, 4.51. Found: C, 48.42; H, 2.48; N, 4.53%.

### *2-Oxo-2H-chromene-3-carboxylic acid N′-[2-(4-benzoyl-2,6-dimethyl-phenoxy)-acetyl]-hydrazide*

**8n**: Yield 82%. m.p. 229–232°C; IR (Nujol): 1625 (C=O), 1675 (amide C=O), 3130–3240 $cm^{-1}$ (NH–NH); $^1H$ NMR ($CDCl_3$): $\delta$ 2.2 (s, 3H, Ar–$CH_3$), 2.3 (S, 3H, $CH_3$), 4.6 (s, 2H, $CH_2$), 7.1–8.2 (m, 11H, Ar–H), 8.8 (s, 1H, coumarin Ar–H), 10.2–10.8 (d, 2H, –NHNH); MS: *m/z* 471. Anal. calcd. for $C_{27}H_{22}N_2O_6$: C, 68.93; H, 4.71; N, 5.95. Found: C, 68.99; H, 4.77; N, 5.96%.

### *2-Oxo-2H-chromene-3-carboxylic acid N′-{2-[4-(2,6-dichloro-benzoyl)-2-methyl-phenoxy]-acetyl}-hydrazide*

**8o**: Yield 70%. m.p. 215–219°C; IR (Nujol): 1625 (C=O), 1675 (amide C=O), 3130–3240 $cm^{-1}$ (NH–NH); $^1H$ NMR ($CDCl_3$): $\delta$ 2.3 (s, 3H, Ar–$CH_3$), 4.4 (s, 2H, $CH_2$), 7.4–8.3 (m, 10H, Ar–H), 8.6 (s, 1H, coumarin Ar–H), 10.2–10.7 (d, 2H, –NHNH); MS: *m/z* 526. Anal. calcd. for $C_{26}H_{18}Cl_2N_2O_6$: C, 59.44; H, 3.45; N, 5.33. Found: C, 59.49; H, 3.50; N, 5.38%.

## Biology

### Cell culture and *in vitro* compounds treatment

MCF-7 breast cancer cells were procured from National Centre for Cell Sciences (NCCS), Pune, India. MCF-7 cells were

 

routinely maintained in DMEM (Sigma, St. Louis, MO, USA) supplemented with 10% heat-inactivated FCS (Himdeia, Mumbai). The EAT cells were collected from JSS College of Pharmacy, Mysore.

### Trypan blue dye exclusion assay

The effect of compounds **8a–o** on the viability of MCF-7 breast cancer cells was determined by Trypan blue dye exclusion assay [3]. MCF-7 breast cancer cells treated with or without compounds were harvested and resuspended in 0.4% Trypan blue and the viable cells were counted using hemocytometer. $IC_{50}$ values were estimated after 48 h of treatment.

### MTT assay

The effect of compounds **8a–o** on cell proliferation of MCF-7 breast cancer cells was determined by MTT assay as described previously [3]. Cells treated with or without compounds were incubated for 48 h. MTT reagent (5 mg/mL) was added and the color change due to proliferating cells was estimated.

### Choriallanotoic membrane (CAM) assay

Inhibition of neovessel formation following the treatment with compounds **8d**, **8l**, and **8o** (10 μM) in fertilized egg CAM was analyzed [4] and changes in the microvessel density were photographed by using Nikon D3200 camera.

### Giemsa and acridine orange/ethidium bromide staining

EAT cells were obtained from the JSS College of Pharmacy, Mysore. The cells were centrifuged at 3000 rpm for 5 min and the packed cells were diluted 1:6 times with phosphate buffer saline. Two milliliters of the diluted cells were treated with the synthesized compounds **8d**, **8l**, and **8o** and incubated for 4 h at 37°C. Untreated EAT cells served as control. At the end of 4 h, the samples were centrifuged, smears were made from the cell pellet obtained and fixed with methanol/acetic acid (3:1), and the morphological features of the cells were observed using different stains. Batches of both test and control smears were stained with Giemsa's stain and acridine orange/ethidium bromide stain that highlights the apoptotic morphology of the cells when observed under bright field microscope and fluorescent microscope, respectively [25].

### DNA fragmentation assay

DNA was isolated from both treated and untreated cells after the incubation of EAT cells with compounds for 4 h. Reactions were terminated using ice-cold Hank's balanced salt solution (HBSS) and the supernatant was discarded after centrifugation. Cells were lysed with 50 mM Tris–HCl buffer, pH 8.0, and 0.5% SDS, which was incubated for 30 min at 37°C. The cell lysate was subjected to 8 M potassium acetate precipitation and left for 1 h at 4°C. The supernatant was subjected to phenol/chloroform/isoamyl alcohol (25:24:1) extraction and chloroform extraction. DNA was precipitated by adding 1:2 vol. of ice-cold ethanol. The precipitated DNA was dissolved in 50 μL of TE buffer (pH 8.0). The DNA was digested with 20 μL/mL of RNase at 37°C for 1 h. The DNA was quantified and equal concentration of DNA (50 μg) was resolved on 1.5% agarose gel, viewed under UV light, and documented using Bio-RAD.

### PI3 kinase assay

The cells were washed with PBS and lysed in lysis buffer. Protein concentrations were determined by bicinchoninic acid protein assay. Lysates (400 μg of protein) were incubated with the substrate at 4°C overnight, followed by further incubation with protein. After the incubation, PI3K assays were performed as per the manufacturer's instructions (PI3K AlphaScreen Assay kit, Echelon Biosciences). The proximity of the interaction between the donor and acceptor was read at a luminescent signal of 600 nm using a plate reader (Table 2).

### Caspase activation assay

Activated caspase was estimated using fluorimetric homogeneous caspase assay (Roche) as per manufacturer's protocol. Briefly, $1 \times 10^4$ cells/well were seeded in 100 μL DMEM supplemented with 10% FBS in each well of 96-well microculture plates and incubated for 24 h at 37°C in a $CO_2$ incubator. After treatment, caspase substrate was added to pre-diluted incubation buffer and incubated for 2 h at 37°C. The developed fluorochrome was proportional to the concentration of activated caspase, which was determined fluorimetrically in the form of free R110 at $\lambda_{max} = 521$ nm.

### Molecular docking

The caspases 1, 3, and 8 and PI3K of human have been associated with tumorigenesis and apoptotic characteristics in cancer. The crystal structure of caspases 1, 3, and 8 was studied, which are responsible for the activation of the corresponding precursor with PDB: 2HBZ, PDB: 4DC, and PDB: 1QDU, respectively. Further crystal structure of PI3K (accession: CAA03853.1) was built using CPH models server 3.0. Energy computations were performed on the molecule using GROMOS96 implementation of Swiss-PDB viewer. Electrostatic point charges on the molecules were calculated. The ligand was docked into the active site using the molecular docking software PATCH Dock with default parameters. PATCH Dock is an algorithm for calculating the docking modes of small molecules into protein-binding sites based on their shape complementarities. In this, we have used ChemScore, a scoring function that is derived from regression against receptor–ligand binding free energies.

 

### Statistical analysis

All experiments were repeated in triplicates in three independent sets. Data are expressed as mean value ± standard deviation (SD). The comparisons between mean values were tested using Duncan's new multiple-range test at a level of $p \leq 0.05$.

*V. Lakshmi Ranganatha gratefully acknowledges the financial support provided by the Department of Science and Technology, New Delhi, under INSPIRE-Fellowship scheme (IF110555). And all authors are thankful to the Principal, Yuvaraja's College, University of Mysore, the Director of Mahajana Research Foundation, Mahajana Education Society, and Head of the Department of Biotechnology, for their support and encouragement throughout the execution of this work. Finally we extend our sincere thanks to Prof. Aravind Balaji for language corrections.*

*The authors have declared no conflict of interest.*

## References

[1] S. Eckhardt, *Curr. Med. Chem.* **2002**, *3*, 419–439.

[2] W. A. Berg, J. D. Blume, J. B. Cormack, E. B. Mendelson, D. Lehrer, M. Böhm-Vélez, E. D. Pisano, R. A. Jong, W. P. Evans, M. J. Morton, M. C. Mahoney, L. H. Larsen, R. G. Barr, D. M. Farria, H. S. Marques, K. Boparai, *JAMA* **2008**, *18*, 2151–2163.

[3] B. T. Prabhakar, S. A. Khanum, K. Jayashree, B. P. Salimath, S. Shashikanth, *Bioorg. Med. Chem.* **2006**, *14*, 435–446.

[4] B. T. Prabhakar, S. A. Khanum, S. Shashikanth, B. P. Salimath, *Invest. New Drugs* **2006**, *24*, 471–478.

[5] J. Shankar, P. B. Thippegowda, S. A. Khanum, *Biochem. Biophys. Res. Commun.* **2009**, *387*, 223–228.

[6] H. D. Gurupadaswamy, V. Girish, C. V. Kavitha, Sathees C. Raghavan, Shaukath Ara Khanum, *Eur. J. Med. Chem.* **2013**, *63*, 536–543.

[7] R. S. Kerbal, *Bioassays* **1991**, *13*, 31–36.

[8] T. Boehm, J. Folkman, T. Browder, M. S. O'Reilly, *Nature* **1997**, *390*, 404–407.

[9] G. E. Henry, H. Jacobs, C. M. S. Carrington, S. Mclean, W. F. Reynolds, *Tetrahedron* **1999**, *55*, 1581–1596.

[10] F. Karrer, H. Meier, A. Pascual, *J. Fluor. Chem.* **2000**, *10*, 381–384.

[11] H. P. Hsieh, J. P. Liou, Y. T. Lin, N. Mahindroo, J. Y. Chang, Y. N. Yang, S. S. Chern, U. K. Tan, C. W. Chang, T. W. Chen, C. H. Lin, Y. Y. Chang, C. C. Wang, *Bioorg. Med. Chem. Lett.* **2003**, *13*, 101–105.

[12] J. P. Liuo, C. W. Chang, J. S. Song, Y. N. Yang, C. F. Yeh, H. Y. Tseng, Y. K. Lo, Y. L. Chang, C. M. Chang, H. P. Haiesh, *J. Med. Chem.* **2002**, *45*, 2556–2562.

[13] Y. Nakagawa, T. Suzuki, *Chem. Biol. Interact.* **2002**, *139*, 115–128.

[14] L. Revesz, E. Blum, F. E. Di Padova, T. Buhl, R. Feifel, H. Gram, P. Hiestand, U. Manning, G. Rucklin, *Bioorg. Med. Chem. Lett.* **2004**, *14*, 3601–3605.

[15] M. Schlitzer, M. Bohm, I. Sattler, *Bioorg. Med. Chem.* **2002**, *10*, 615–620.

[16] S. Iyer, D. J. Chaplin, D. S. Rosenthal, A. H. Boulares, L. Y. Li, M. E. Smulson, *Cancer Res.* **1998**, *58*, 4510–4514.

[17] K. Balasubramanyam, M. Altaf, A. V. Radhika, V. Swaminathan, R. Aarthi, P. Parag, T. P. Sadhal Kundu, *J. Biol. Chem.* **2004**, *279*, 33716–33726.

[18] J. R. Hoult, M. Paya, *Gen. Pharm.* **1996**, *27*, 713–722.

[19] M. Marshall, K. Kervin, C. Benefield, A. Umerani, S. Albainy-Jenei, Q. Zhao, M. Khazaeli, *J. Cancer Res. Clin. Oncol.* **1994**, *120*, 39–42.

[20] V. Reutrakul, P. Leewanich, P. Tuchinda, M. Pohmakotr, T. Jaipetch, S. Sophasan, T. Santisuk, *Planta Med.* **2003**, *69*, 1048–1051.

[21] S. A. Khanum, A. Bushra begum, V. Girish, N. F. Khanum, *Int. J. Biomed. Sci.* **2010**, *6*, 60–65.

[22] S. A. Khanum, V. Girish, S. S. Suparshwa, N. F. Khanum, *Bioorg. Med. Chem. Lett.* **2009**, *19*, 1887–1891.

[23] V. Lakshmi Ranganatha, N. Vinutha, Shaukath A. Khanum, Sumati Anthal, D. Revannasiddaiah, Rajnikant, K. Vivek Gupta, *X-Ray Struct. Anal. Online* **2012**, *28*, 27–28.

[24] H. D. Gurupadaswamy, V. Girish, C. V. Kavitha, Sathees C. Raghavan, Shaukath Ara Khanum, *Eur. J. Med. Chem.* **2013**, *63*, 536–543.

[25] G. Srinivas, R. John Anto, P. Srinivas, S. Vidhyalaxmi, V. PriyaSenan, D. Karunagaran, *Eur. J. Pharmacol.* **2003**, *473*, 117–125.

 